THE JOURNAL OF BIOLOGICAL CHEMISTRY VOL. 282, NO. 40, pp. 29531–29539, October 5, 2007

Phosphorylation Blocks the Activity of Tubulin Polymerization-promoting Protein (TPPP)

*IDENTIFICATION OF SITES TARGETED BY DIFFERENT KINASES**

Received for publication, April 25, 2007, and in revised form, July 31, 2007 Published, JBC Papers in Press, August 11, 2007, DOI 10.1074/jbc.M703466200

Emma Hlavanda[‡1], Eva Klement[§1], Endre Kókai[¶], János Kovács[‖], Orsolya Vincze[‡], Natália Tőkési[‡], Ferenc Orosz[‡], Katalin F. Medzihradszky[§], Viktor Dombrádi[¶], and Judit Ovádi[‡2]**

*From the [‡]Institute of Enzymology, Biological Research Center, Hungarian Academy of Sciences, Budapest, H-1113, Hungary, the [§]Proteomics Research Group, Biological Research Center, Hungarian Academy of Sciences, H-6726 Szeged, Hungary, the [¶]Cell Biology and Signaling Research Group of the Hungarian Academy of Sciences, Department of Medical Chemistry, Research Center for Molecular Medicine, University of Debrecen, Debrecen, H-4032, Hungary, the [‖]Department of Anatomy, Cell and Developmental Biology, Faculty of Sciences, University of Eötvös Loránd, Budapest, H-1117 Hungary, and the **Department of Pharmaceutical Chemistry, University of California/San Francisco, San Francisco, California 94143-0446*

Tubulin polymerization-promoting protein (TPPP), an unfolded brain-specific protein interacts with the tubulin/microtubule system *in vitro* and *in vivo*, and is enriched in human pathological brain inclusions. Here we show that TPPP induces tubulin self-assembly into intact frequently bundled microtubules, and that the phosphorylation of specific sites distinctly affects the function of TPPP. *In vitro* phosphorylation of wild type and the truncated form (Δ3-43TPPP) of human recombinant TPPP was performed by kinases involved in brain-specific processes. A stoichiometry of 2.9 ± 0.3, 2.2 ± 0.3, and 0.9 ± 0.1 mol P/mol protein with ERK2, cyclin-dependent kinase 5 (Cdk5), and cAMP-dependent protein kinase (PKA), respectively, was revealed for the full-length protein, and 0.4–0.5 mol P/mol protein was detected with all three kinases when the N-terminal tail was deleted. The phosphorylation sites Thr[14], Ser[18], Ser[160] for Cdk5; Ser[18], Ser[160] for ERK2, and Ser[32] for PKA were identified by mass spectrometry. These sites were consistent with the bioinformatic predictions. The three N-terminal sites were also found to be phosphorylated *in vivo* in TPPP isolated from bovine brain. Affinity binding experiments provided evidence for the direct interaction between TPPP and ERK2. The phosphorylation of TPPP by ERK2 or Cdk5, but not by PKA, perturbed the structural alterations induced by the interaction between TPPP and tubulin without affecting the binding affinity (K_d = 2.5–2.7 μM) or the stoichiometry (1 mol TPPP/mol tubulin) of the complex. The phosphorylation by ERK2 or Cdk5 resulted in the loss of microtubule-assembling activity of TPPP. The combination of our *in vitro* and *in vivo* data suggests that ERK2 can regulate TPPP activity via the phosphorylation of Thr[14] and/or Ser[18] in its unfolded N-terminal tail.

Previously we isolated a new, flexible, intrinsically unstructured protein from bovine brain, which was denoted tubulin polymerization-promoting protein (TPPP)[3]/p25 accordingly to its *in vitro* function, tubulin polymerization-promoting protein, and its molecular mass (1). In the HGNC data base this protein is assigned as TPPP, the first member of TPPP family. We have shown that TPPP can induce formation of double-walled microtubules (MTs) and aberrant tubulin aggregates (2) as well as that it stabilizes MT network via its bundling activity in human cells (3). There are two TPPP homologues, p18 (TPPP2) and p20 (TPPP3) with distinct structural and functional features concerning their folding and tubulin binding properties (4). The physiological functions of the TPPP protein family are unknown; however, TPPP has been suggested to take part in the stabilization of the MT network (3).

Both α-synuclein and GAPDH directly bind to TPPP and co-localize in the Lewy body (5–7). Our immunohistochemistry studies revealed enrichment of TPPP in α-synuclein-positive inclusions characteristic for synucleinopathies but not for tauopathies (5). TPPP is similar to α-synuclein and tau (2, 8) as far as all of them belong to the family of the unstructured proteins.

Protein phosphorylation has a significant impact in the etiology of neurodegenerative processes (9). For example, tau and α-synuclein, the major hallmarks of Parkinson and Alzheimer diseases, respectively, are targets of different protein kinases. One of the kinases phosphorylating tau with pathological relevance in Alzheimer disease is cyclin-dependent kinase 5 (Cdk5), which is abundant in brain tissue, associates with tau (10), and plays important role in the signaling of mitogen-activated protein kinases (MAP kinases) also called extracellular signal-regulated kinases (ERKs). MAP kinases and Cdk5 phos-

* This work was supported in part by Hungarian National Scientific Research Fund Grants OTKA T-046071 (to J. O.) and T-049247 (to F. O.), by the Hungarian National Office for Research and Technology Grant RET-08/2004 (to K. F. M.), FP6-2003-LIFESCIHEALTH-I: Bio-Sim, and NKFP-MediChem2 1/A/005/2004 (to J. O.). The costs of publication of this article were defrayed in part by the payment of page charges. This article must therefore be hereby marked "*advertisement*" in accordance with 18 U.S.C. Section 1734 solely to indicate this fact.

[1] These authors contributed equally to the work.

[2] To whom correspondence should be addressed: Inst. of Enzymology, Biological Research Center, Hungarian Academy of Sciences, Budapest, Karolina út 29, H-1113, Hungary. Fax: 36-1-4665465; E-mail: ovadi@enzim.hu.

[3] The abbreviations used are: TPPP, tubulin polymerization-promoting protein; MT, microtubule; TEM, transmission electron microscopy; ERK2, extracellular signal-regulated protein kinase 2; PKA, cAMP-dependent protein kinase; Cdk5, cyclin-dependent kinase 5; MAP, microtubule-associated protein; PSD, post source decay; CID, collision-induced dissociation; DTT, dithiothreitol; MOPS, 4-morpholinepropanesulfonic acid; MES, 4-morpholineethanesulfonic acid; GAPDH, glyceraldehyde-3-phosphate dehydrogenase.

phorylate numerous KSP*X*K consensus motifs in diverse cytoskeletal proteins and cross-talk in the regulation of neuronal functions (11). The cAMP-dependent protein kinase (PKA) interacts with the so-called A kinase-anchoring proteins via its regulatory subunit, that targets the kinase activity to specific subcellular locations (12) including MTs through a direct binding to MAP2 (13, 14).

Currently there is limited information on the phosphorylation of TPPP, although it has been considered as a phosphoprotein (15). It was partially co-purified with tau protein kinase II (also denoted Cdk5) from bovine brain extract; and two of the Ser/Thr-Pro sites in synthetic peptides, segments of TPPP, were phosphorylated by Cdk5 (15). Martin *et al.* (16) suggested that rat brain TPPP could be phosphorylated near to stoichiometrically *in vitro* by Cdk5 and by PKA but practically not by glycogen synthase kinase 3.

The aim of this work was to demonstrate that TPPP was able to promote the formation of intact-like MTs exhibiting a function characteristic of MAPs, and to establish the effect of phosphorylation on the unfolded "structure" of TPPP, on its interaction with tubulin as well as on its MT promoting and bundling activities. For these purposes we performed *in vitro* phosphorylation studies with human recombinant TPPP and with its truncated form, searched for the *in vivo* phosphorylation sites and interacting kinase partner(s), as well as studied the functional consequences of the specific phosphorylation events.

EXPERIMENTAL PROCEDURES

Materials—DTT, iodoacetamide, NH_4HCO_3, and 2,5-dihydroxybenzoic acid were obtained from Sigma, the sequencing grade side-chain protected trypsin (modified by reductive methylation) was ordered from Promega. C18 ZipTip was from Millipore. MAP-free tubulin was purified from bovine brain as described in Ref. 17. Ni-NTA magnetic agarose beads were purchased from Qiagen. TiO_2 was from SunChrom GmbH.

An active complex of N-terminal His-tagged human Cdk5 and N-terminal glutathione *S*-transferase-tagged human p25 protein was obtained from Upstate Biochemicals. The two proteins were co-expressed in baculovirus-infected Sf21 insect cells. The catalytic subunit of PKA isolated from bovine heart was from Calbiochem. The catalytic subunit was active without the addition of cAMP. His-tagged activated human ERK2 expressed in *Escherichia coli* was from Calbiochem. [γ^{32}P]ATP was purchased from the Institute of Isotopes. Fine chemicals and buffer components were from Sigma.

DNA Manipulations—The coding region of human TPPP (5) was inserted into the XhoI and BamHI restriction sites of pET15b vector (Novagen) producing pET15b-TPPP. A PCR fragment for expression of Δ3-43TPPP, the deletion mutant lacking residues 3-43, was generated using pET15b-TPPP as template with the following primers: 5′-GATACTCGAGATGGCTGCATCCCCTGAGCTCAGTGCCCTGGAGGAG-3′ and 5′-CCGTGGATCCCTACTTGCCCCCTTGCACCTTCTGGTCGTAGG-3′. The PCR fragment was inserted into the XhoI and BamHI restriction sites of pET-15b producing pET15b-Δ3-43TPPP. Correct ligations were verified by DNA sequencing.

Protein Purification—Recombinant human TPPP and p20 (TPPP3) were expressed in *E. coli* BL21 (DE3) cells and isolated as described previously (4, 5). Δ3-43TPPP was expressed in *E. coli* and was purified on HIS-Selected™ Cartridge (Sigma H8286) as the full-length TPPP.

Protein Determination—The protein concentration was measured by the Bradford method (18) using the Bio-Rad protein assay kit.

Affinity Chromatography—Human recombinant TPPP was immobilized to CNBr-activated Sepharose 4B (Amersham Biosciences) and used for finding interacting proteins from bovine brain extract as described previously (6). The bound proteins were eluted with 10 mM phosphate buffer, pH 7.0, containing 0.5 M NaCl, and the protein bands obtained by SDS-PAGE (19) were analyzed by mass spectrometry.

Protein Phosphorylation—30 μg of recombinant human TPPP or its truncated form (Δ3-43TPPP) or p20 protein (TPPP3) were phosphorylated with PKA, ERK2, and Cdk5 *in vitro*. A typical reaction mixture contained 50 mM Tris-HCl; pH 7.5 buffer supplemented with 1 mM benzamidine, 1 mM phenylmethylsulfonyl fluoride, 1 mM EGTA, 10 mM NaF, 0.05 mM sodium vanadate, 25 mM $MgCl_2$, 0.2 mM ATP, and 0.4 μg PKA or 0.2 μg of ERK2 in a final volume of 100 μl. In one set of experiments 30 μg of recombinant human TPPP was phosphorylated with 0.1 μg of ERK2 to reduce the degree of modification. Phosphorylation with Cdk5 was conducted in the presence of 12 mM MOPS, pH 7.0 buffer, 0.2 mM EDTA, 1 mM EGTA, 5 mM NaF, 0.2 mM sodium vanadate, 0.2 mM dithiothreitol, 27 mM $MgCl_2$, 0.2 mM ATP, and 0.05 μg of kinase. About 10^7 cpm of [γ-^{32}P]ATP was added to the mixture for radioactive labeling. The reactions were initiated by the addition of the kinase and were terminated with 50 mM EDTA. 5-μl samples were withdrawn at regular time intervals for quantitative analysis. Phosphate incorporation into the proteins was determined by the method of Witt and Roskoski (20) using Whatmann P-81 filter paper. The radioactivity was counted by Tscherenkov radiation. Aliquots of the samples were separated by SDS-PAGE (19). Dried gels were analyzed by autoradiography using RX Fuji medical x-ray films. According to the densitometric scanning of the films with a Bio-Rad Multi-Analyst apparatus more than 90% of the incorporated radioactivity was found in the monomeric and dimeric forms of the proteins. A prestained protein ladder (Fermentas) was used for the estimation of the molecular masses. Radioactive and cold phosphorylation reactions were run parallel under identical conditions. The degree of phosphorylation in the latter case was checked by the method of back phosphorylation (21). Only the non-radioactive samples were subjected to functional studies and MS.

In-gel Digestion—Digestion with side chain-protected porcine trypsin proceeded at 37 °C for 4 h.

In-solution Digestion—Protein was dissolved in 6 M guanidine-HCl, disulfide bridges were reduced with dithiothreitol and free sulfhydryls alkylated with iodoacetamide. Then sample was diluted with 25 mM NH_4HCO_3 and digested with side chain-protected porcine trypsin at 37 °C for 4 h.

Methyl Esterification—The protocol of Ficarro (22) was applied.

Phosphopeptide Enrichment by Immobilized Metal Ion Affinity Chromatography—In NTA magnetic agarose beads Ni^{2+} was displaced by Fe^{3+} as described by Thompson *et al.* (23) with final washing steps with a mixture of equal volumes of water, methanol, and acetonitrile. Methyl-esterified sample dissolved in water/methanol/acetonitrile was loaded onto the beads and vortexed for 15 min, then beads were washed three times with the loading solvent. Phosphopeptides were eluted with 0.42% H_3P0_4 in 50% acetonitrile. An aliquot of the eluate was either directly analyzed by MALDI-TOF MS or diluted with 0.1% formic acid and loaded on the trapping column for LC-MS/MS.

Phosphopeptide Enrichment by TiO_2—A modified protocol of Larsen *et al.* (24) was applied. The tryptic digest was dried down, re-dissolved in 1% trifluoroacetic acid/50% acetonitrile and mixed with TiO_2 suspended in the same solvent. After a few minutes vortexing the supernatant was discarded, and TiO_2 was washed three to five times with the same solvent. Phosphopeptides were eluted with 1% NH_4OH.

MALDI-TOF MS and PSD Analysis—These analyses were performed on a Bruker Reflex III MALDI-TOF mass spectrometer in 2,5-dihydroxy-benzoic acid matrix. Three point external calibration was used with standard peptides. PSD analysis was performed in 10–12 steps, lowering the reflectron voltage by 25% at each step, and then stitching the data together. While the MS conditions permitted monoisotopic mass measurements, in PSD mode average masses were determined.

LC-MS/MS—Samples were analyzed on an Agilent 1100 nanoLC system on-line coupled to an XCT Plus ion trap mass spectrometer in information-dependent acquisition mode. For phosphopeptide analysis, occasionally a preferred mass list was included in data acquisition with m/z values calculated from MALDI-TOF data or derived from previous analyses. HPLC conditions were as follows: column: C18, 75 μm × 150 mm; flow rate 300 nl/min; gradient: 5–45% B in 16 min, up to 90% B for 3 min, then equilibrated at 5% B for 15 min; solvent A was 0.1% formic acid in water, solvent B: 0.1% formic acid in acetonitrile; trapping: 10 μl/min flow rate, for 5 min in solvent A.

Data Base Search—MS and MS/MS data were searched against the Swissprot 51.3 (250,296 sequences) and the NCBI 20070120 (4462937 sequences) non-redundant protein databases using the Mascot search engine v2.1. Mass tolerance was set according to the type of instrument and acquisition mode. No species restriction was used. Data were also manually inspected.

Bioinformatic Methods—For prediction of phosphorylation and docking sites MotifScan (25) was used. Multiple sequence alignment of vertebrate TPPPs was done by ClustalW (26).

CD Measurements—CD spectra were acquired with a Jasco J-720 spectropolarimeter (Tokyo, Japan) in the 190–260 nm wavelength range employing 0.1-cm thermostated cuvettes at 25 °C, using 10 mM phosphate buffer (pH 7.0) as described previously (4). During the titration of 1 μM tubulin the difference ellipticity at 207 nm was determined as a function of the concentration of TPPP. Difference ellipticities were calculated from the ellipticity measured at 207 nm in the mixtures of two proteins and in the samples of the individual proteins.

Turbidity Measurements—A total of 7 μM MAP-free tubulin was polymerized by 3 μM TPPP before and after phosphorylation at 37 °C in 50 mM MES buffer, pH 6.6, containing 1 mM dithiothreitol, 1 mM EDTA, 1 mM $MgCl_2$, and 50 mM KCl. In the absence of TPPP no tubulin assembly occurs. Absorbance was monitored at 350 nm by a Cary 50 spectrophotometer (Varian, Australia).

Transmission Electron Microscopy (TEM)—The polymerized tubulin samples were centrifuged at 30,000 × *g* and 30 °C for 20 min and the pellet fraction was used for TEM. The pellets were fixed for 1 h in a mixture of 2% glutaraldehyde, 0.2% freshly prepared tannic acid, and 0.1 M sodium cacodylate (pH 7.4). After washing in cacodylate, they were postfixed in 0.5% OsO_4, and embedded in Durcupan (Fluka, Switzerland). Thin sections were contrasted with uranyl acetate and lead citrate and examined in a Jeol CX 100 electron microscope (1).

RESULTS

In Vitro Phosphorylation of TPPP—Recombinant human TPPP was phosphorylated by protein kinases (ERK2, Cdk5, and PKA) in the presence of [γ-^{32}P]ATP under conditions to reach maximal phosphorylation within 2 h (see "Experimental Procedures"). Fig. 1 shows typical SDS/PAGE protein staining and autoradiographic images. Two characteristic phosphoprotein bands of 26.5 and 63 kDa appeared in the pictures corresponding to monomeric and dimeric species. By the addition of an excess DTT to the samples all of the dimers were converted to monomers (data not shown). The radioactivity incorporated into TPPP was determined as described under "Experimental Procedures"; the stoichiometry of the phosphorylation was found to be 2.9 ± 0.3, 2.2 ± 0.3, and 0.9 ± 0.1 mol P/mol protein for ERK2, Cdk5, and PKA kinases, respectively (Fig. 1).

The phosphorylated protein bands were excised from the gels and digested with trypsin. After phosphopeptide enrichment, samples were analyzed by MALDI-TOF MS, MALDI-TOF PSD, and by LC-MS/MS on an ion trap mass spectrometer. Phosphopeptides were first identified by the 80-Da mass shift in comparison to the predicted molecular masses of tryptic peptides. Their identity was further confirmed by the β-elimination of phosphoric acid (98 Da) from the precursor ion under collision-induced dissociation (CID) or post source decay (PSD) conditions, a characteristic fragmentation step of Ser- and Thr-phosphorylated peptides (27). The sites of phosphorylation were assigned considering the 80 Da mass shift of the appropriate peptide fragments (Table 1).

In agreement with the minimal consensus of ERK2 and Cdk5, Ser, and Thr residues followed by Pro were targeted by these kinases. From the total of 4 such sites in TPPP, Ser^{18}, and Ser^{160} were phosphorylated by ERK2, while Thr^{14}, Ser^{18}, and Ser^{160} were modified by Cdk5. PKA phosphorylated Ser^{32} within the single PKA consensus sequence KRLS in addition to Thr^{92} and Ser^{159} residues, which are in a less favorable sequence environment and may represent minor or unspecific sites. Therefore,

we conclude that under *in vitro* conditions Thr[14], Ser[18], Ser[32], and Ser[160] of human TPPP are the main phosphorylation sites of the MT-associated kinases.

Our structural prediction (8) suggested a quite extended region in the N terminus of TPPP (1–52 amino acids) with highly unfolded structure. As three of the main phosphorylation sites, Thr[14], Ser[18], and Ser[32], are localized in this tail region we expressed a truncated form of the human TPPP that lacks the first 43 amino acid residues (Δ3-43TPPP) and investigated the consequences of this deletion. Fig. 1 demonstrates that the truncation of the protein significantly reduced both the rate and degree of its phosphorylation. A 0.4–0.5 mol of P/mol protein stoichiometry was reached after 2 h of incubation with ERK2, Cdk5, and PKA. As a negative control, the phosphorylation of recombinant human p20 (TPPP3), a homologue of TPPP that lacks the N-terminal tail, and the phosphorylation site corresponding to Ser[160] in TPPP was also tested under similar conditions; and as expected virtually no ^{32}P incorporation (0.02 mol of P/mol protein) was detected. These results suggest that ERK2 and Cdk5 phosphorylate the residues Thr[14] and Ser[18] in the N-terminal tail more vigorously than Ser[160]; and PKA efficiently modifies Ser[32] that is also localized in the N terminus. Our data are consistent with the predictions by MotifScan (25) for the probability of the phosphorylation sites by PKA, ERK2, or Cdk5 (see Table 3).

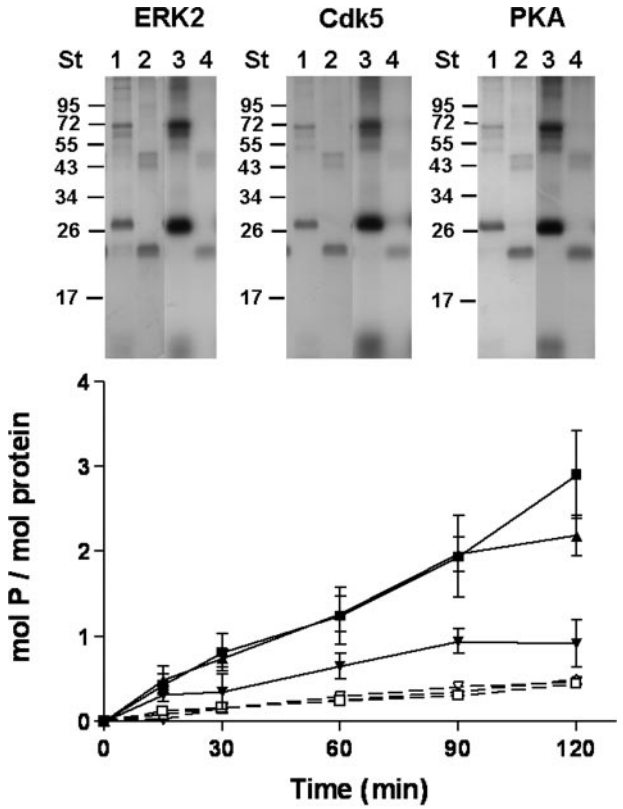

FIGURE 1. ***In vitro* phosphorylation of human TPPP.** Recombinant full-length TPPP (*lanes 1* and *3*) and truncated Δ3-43TPPP (*lanes 2* and *4*) proteins were phosphorylated in the presence of [γ^{32}P]ATP with ERK2, Cdk5, and PKA. Samples taken after 2 h of phosphorylation were separated in 10% SDS/PAGE, stained with Coomassie Brillant Blue (*lanes 1* and *2*), and visualized by autoradiography (*lanes 3* and *4*) using 4 h (ERK2 and Cdk5) or 12 h (PKA) exposure of the photographic films. The positions of the standards (*St*) are marked, and their molecular masses are given in kDa. The *lower panel* shows the time course and stoichiometry of phosphorylation calculated from the radioactivity incorporated into the trichloroacetic acid-insoluble proteins by ERK2 (■, □), Cdk5 (▲, △), and PKA (▼, ▽) as measured with TPPP (*full lines* and *filled symbols*, 4–6 independent experiments) or with Δ3-43TPPP (*broken lines* and *open symbols*, two independent experiments), respectively.

In Vivo Phosphorylation of TPPP—To test if the *in vitro* phosphorylation sites are also relevant under *in vivo* conditions we isolated TPPP from bovine brain as described previously (2), and identified the phosphorylated sites of TPPP by MS. Phosphopeptides detected by MS without or after TiO_2 enrichment are summarized in Table 2. The PSD spectrum of the peptide at $MH^+ = 2954.5$ produced fragments at *m/z* 1165.0 (y_{10}), 1635.2 (y_{16}), 1764.0 (y_{18}), and 2077.2 (y_{22}) revealing phosphorylation at Ser[30]. A series of CID spectra unambiguously identified phosphorylation at Thr[12], as listed in Table 2. Phosphorylation site assignments were based on preferential peptide backbone cleavages between [7]LysPro[8] and [12]ThrPro[13]. Determination of the phosphorylation sites in the doubly phosphorylated Ac-(2–24) peptide was performed from the quadruply charged precursor at *m/z* 655.7 (Fig. 2). The fragment ion observed at *m/z* 665.9 can only be assigned as y_{12}^{2+} with one phosphate in this fragment, *i.e.* phosphorylation at Ser[16]. The fragment ion observed at *m/z* 641.6 corresponds to the doubly phosphorylated y_{17}^{3+} thus confirming an additional phosphate at position Thr[12].

The human and bovine TPPP proteins exhibit >90% homology (1) and carry the same phosphorylation sites, however, because of the deletion of two amino acid residues at the N terminus of the bovine protein the numbering of the phosphorylated residues is shifted (Fig. 3). Therefore, the *in vivo* phosphorylation sites identified in the bovine protein are in agreement with those phosphorylated *in vitro* in human recombinant TPPP (Table 3). Ser[159] in the bovine protein corresponding to Ser[160] in the human ortholog was not found to be phosphorylated *in vivo*.

TABLE 1

Identification of phosphorylation sites in human recombinant TPPP phosphorylated *in vitro* by Cdk5, ERK2, and PKA

Phosphorylated residues are indicated as pX, if MS/MS data enabled exact phosphorylation site determination. Residues are underlined where fragmentation produced y and/or b ions that contributed to phosphorylation site determination. Methyl esterified Asp, Glu, and C-terminal residues are marked with apostrophe.

MH^+	*m/z*	Charge	Sequence	Position	Enrichment	Site	Kinase
998.0	499.5	2+	AIS<u>pSPTVSR</u>	[157–165]	TiO_2	Ser-160	Cdk5, ERK2
1011.6	506.3	2+	AI<u>pSSPTVSR</u>'	[157–165]	Fe-NTA	Ser-159	PKA
1559.0	780.0	2+	NV<u>TVTD</u>'VD'IVFSK'	[90–102]	Fe-NTA	Thr-92	PKA
3081.7	1027.9	3+	RL<u>pSLE</u>'S.E.'<u>GAGE</u>'<u>GAAASPE</u>'LSALE'E'AFRR'	[30–57]	Fe-NTA	Ser-32	PKA
1874.5	625.5	3+	AAN<u>RTPPKpSPGDPSKDR</u>	[10–26]	TiO_2	Ser-18	Cdk5, ERK2
1462.3	488.1	3+	<u>TPPKpSPGDPSKDR</u>	[14–26]	TiO_2	Ser-18	Cdk5, ERK2
1504.3	502.1	3+	<u>TPPKpSPGD'PSKD'R'</u>	[14–26]	Fe-NTA	Ser-18	Cdk5, ERK2
1218.6	609.8	2+	<u>TPPKpSPGD'PSK'</u>	[14–24]	Fe-NTA	Ser-18	Cdk5, ERK2
1915.9	1915.9	1+	AANR<u>pTPPKSPGD'PSKD'R'</u>	[10–26]	Fe-NTA	Thr-14	Cdk5

TABLE 2

***In vivo* phosphorylated peptides identified by MALDI-TOF MS and/or LC-MS/MS in tryptic digests of TPPP isolated from bovine brain**

Phosphorylated residues are indicated as pX, if MS/MS data enabled exact phosphorylation site determination. Residues are underlined where fragmentation produced y and/or b ions that contributed to phosphorylation site determination. All of the peptides were enriched by TiO_2 except for the last modified peptide that was detected by MALDI-TOF MS without enrichment.

MH^+	Precursor m/z	Charge	Sequence	Position	No. of phosphate	Site(s)
2295.2	575.0	4+	Ac-ADSRPKPANKpTPPKSPGEPAK	Ac-[2–22]	1	Thr-12
2410.5	603.6	4+	Ac-ADSRPKPANKpTPPKSPGEPAKD	Ac-[2–23]	1	Thr-12
2410.5	483.1	5+	Ac-ADSRPKPANKpTPPKSPGEPAKD	Ac-[2–23]	1	Thr-12
2538.5	508.9	5+	Ac-ADSRPKPANKpTPPKSPGEPAKDK	Ac-[2–24]	1	Thr-12
2618.5	655.7	4+	Ac-ADSRPKPANKpTPPKpSPGEPAKDK	Ac-[2–24]	2	Thr-12, Ser-16
2680.6	537.1	5+	Ac-ADSRPKPANKpTPPKSPGEPAKDKAA	Ac-[2–26]	1	Thr-12
2680.6	671.0	4+	Ac-ADSRPKPANKpTPPKSPGEPAKDKAA	Ac-[2–26]	1	Thr-12
2760.6	691.3	4+	Ac-ADSRPKPANKTPPKSPGEPAKDKAA	Ac-[2–26]	2	
2808.7	562.7	5+	Ac-ADSRPKPANKTPPKSPGEPAKDKAAK	Ac-[2–27]	1	
2954.9	2954.9	1+	RLpSLEAEGAGEGAAAAGAELSALEEAFRK	[28–56]	1	Ser-30

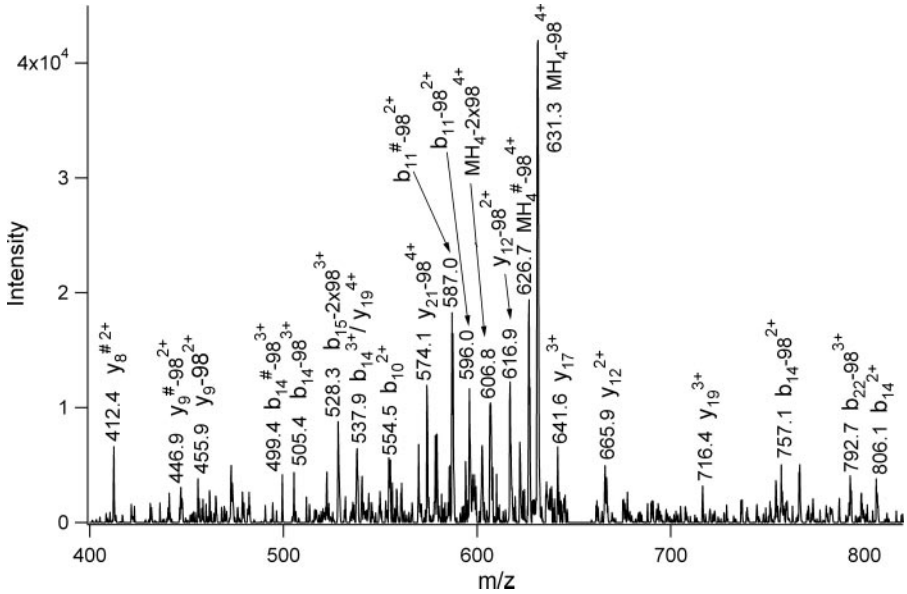

FIGURE 2. **Identification of phospho-Thr[12] and phospho-Ser[16] of TPPP isolated from bovine brain.** CID of the precursor at m/z 655.7 (4+) confirmed the identity of the doubly phosphorylated Ac-ADSRPKPANKpTPP-KpSPGEPAKDK (2–24) peptide. Fragments assigned as y_{12}^{2+} and y_{17}^{3+} unambiguously identified Thr[12] and Ser[16] being phosphorylated.

Interaction of TPPP with ERK2—Next we investigated whether the post-translational modification of TPPP was assisted by a so-called docking mechanism, *i.e.* by a direct interaction between TPPP and the kinase(s). For this purpose affinity binding experiments were carried out by loading a crude bovine brain extract on a TPPP-Sepharose column.

Fig. 4*A* shows the proteins that were bound to the affinity column, and then eluted by 0.5 M NaCl. The two dominant bands in the gel correspond to tubulin and GAPDH as reported earlier (6). Between these two bands the marked band was excised and in-gel digested with trypsin. The digest was analyzed by LC-MS/MS on an ion trap mass spectrometer. In the digest ERK2 (NCBI acc. NP_786987) was identified from the MS/MS spectra of peptides m/z 643.16 (2+), m/z 651.0 (2+) (Fig. 4*B*), and m/z 974.6 (1+) revealing the sequences Ac-AAAAAAGAGPEMVR (2–15), Ac-AAAAAAGAGPE-M(ox)VR (2–15), and GQVFDVGPR (16–24), respectively. In addition, MotifScan (25) analysis predicted ERK docking sites in TPPP, one of them containing the characteristic L*X*L sequence motif (28) in the N-terminal region. The finding that ERK2 can directly bind to TPPP underlines the significance of this kinase in the post-translational modification of Ser/Thr-Pro residues in TPPP.

Effect of Phosphorylation on the Interaction of TPPP with Tubulin—As shown in Fig. 5*A*, the human recombinant TPPP displays a CD spectrum with a minimum at 205 nm that is characteristic for the unstructured proteins. We found that phosphorylation by ERK2, Cdk5, or PKA did not perturb the CD spectrum (data not shown) indicating that the phosphorylation did not elicit detectable changes in the secondary structure of the protein. We confirmed our previous data (2) that the addition of tubulin to TPPP altered the CD spectrum significantly, and demonstrated that the phosphorylation of TPPP by ERK2 with a stoichiometry of 2.9 P/mol protein modified the spectrum of the TPPP-tubulin complex (Fig. 5*A*). The phosphorylation decreased the binding-induced structural changes (the difference of the ellipticity obtained with the mixture compared with the sum of the individual proteins). The phosphorylation of TPPP by Cdk5 (2.2 P/mol protein) had a similar effect, while the phosphorylation with PKA (0.9 P/mol protein) had no effect (data not shown). Thus our data suggest that ERK2 or Cdk5 can perturb the interaction of TPPP with tubulin, in contrast to PKA that is ineffective in this respect.

For the evaluation of the role of phosphorylation on the characteristics of the TPPP-tubulin interaction, the ellipticity differences were determined from the CD spectra measured at varying concentrations of TPPP before and after its phosphorylation. Fig. 5*B* shows that although the phosphorylation significantly reduced the difference ellipticity at the saturation levels (characteristic for the secondary structure elements), the dissociation constants (K_d = 2.5–2.7 μM) and the stoichiometry (~1 mol TPPP/mol tubulin) estimated from the Wu-Hammes plots were not changed significantly (Fig. 5*C*).

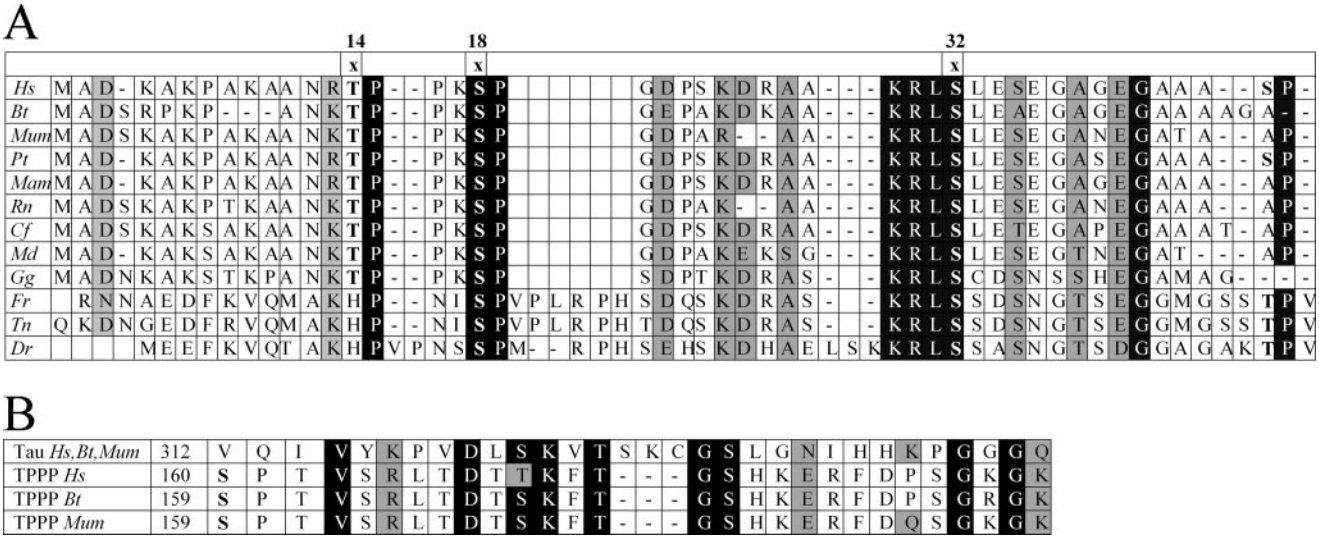

FIGURE 3. *A*, multiple sequence alignment of the N-terminal tail of vertebrate TPPPs by ClustalW (26) *Hs*, *Homo sapiens*; *Bt*, *Bos taurus*; *Mum*, *Mus musculus*; *Pt*, *Pan troglydes*; *Mam*, *Macaca mulatta*; *Rn*, *Rattus norvegicus*; *Cf*, *Canis familiaris*; *Md*, *Monodelphis domestica*; *Gg*, *Gallus gallus*; *Fr*, *Fugu rubripes*; *Tn*, *Tetraodon nigroviridis*; *Dr*, *Danio rerio*. Residues identical and similar in all species are indicated by *black* and *gray backgrounds*, respectively. Putative phosphorylation sites are indicated with *bold characters*. Amino acid residues found to be phosphorylated *in vivo* or *in vitro* are labeled with *x* (see Table 3). The numbering refers to the human TPPP. *B*, alignment of TPPP with one of the MT binding sites of tau protein. *Hs*, *H. sapiens*; *Bt*, *B. taurus*; *Mum*, *M. musculus*. This part of the sequence of tau is identical in the three species. Residues identical with and similar to the tau amino acid residues are indicated by *black* and *gray backgrounds*, respectively.

TABLE 3
Summary of the phosphorylation sites in TPPP

Kinases	Phosphorylated sites											
	Thr			Ser			Ser			Ser		
	b[a] 12	h[b] 14	m[c] 15	b 16	h 18	m 19	b 30	h 32	m 31	b 159	h 160	m 159
Probability[d]												
CDK5		Medium			Medium						Low	
ERK2		Low			Medium						Low	
PKA								High				
In vitro												
CDK5		+			+[e] +						+[e] +	
ERK2					+						+	
PKA								+				
In vivo		+ +[f] +[f]			+ +[f] +[f]			+ +[f] +[f]				

[a] b, bovine.
[b] h, human.
[c] m, mouse.
[d] Probability of phosphorylation predicted by MotifScan. High stringency indicates that the motif identified in the query sequence is within the top 0.2% of all matching sequences contained in vertebrate Swiss-Prot protein database. Medium and low stringency scores correspond to the top 1% and 5% of sequence matches, respectively.
[e] Peptide phosphorylation (15).
[f] Phosphoproteomics (30–32).

Assembly of MTs Induced by TPPP and the Effect of Phosphorylation on This Process—Previously we reported that TPPP promotes tubulin polymerization into aberrant, sometimes double-walled, tubules as well as into large aggregates (1). Now we found the conditions at which TPPP was able to induce the formation of intact-like MTs. The addition of 3 μM TPPP to 7 μM MAP-free tubulin in the polymerization buffer at 37 °C induced tubulin polymerization as detected by turbidimetry (Fig. 5*D*). TEM analysis of the pellet fraction revealed the appearance of large amounts of MTs, ~25–26 nm in diameter, the majority of which formed bundles consisting of dozens of MTs (Fig. 6*A*). The MTs were frequently decorated by rows of tiny projections and dense particles with a periodicity of about 16 nm. The particles appear to connect MTs in the bundle (Fig. 6*B*). These pictures provide the first experimental evidence that TPPP induces intact-like MTs. Another characteristic morphological feature of these samples, beside the single and bundled MTs, is the presence of thread-like oligomers. The threads are ~15 nm in diameter and are concentrated in densely packed knobs between the bundles of MTs (Fig. 6*A*).

The effect of phosphorylation on the ability of TPPP to promote tubulin polymerization was also analyzed by time-dependent turbidity measurements. In contrast to the control (no phosphorylation) the ERK2-mediated modification of TPPP (2.9 mol P/mol protein) completely blocked tubulin polymerization (Fig. 5*D*). The inhibition was so extensive that prevented a TEM analysis, as it was impossible to collect polymerized species by centrifugation. The Cdk5-mediated phosphorylation diminished the assembly activity of TPPP as well, however, PKA was ineffective (data not shown).

We tested whether a partially phosphorylated TPPP maintained any MT assembling activity. In a specific set of experi-

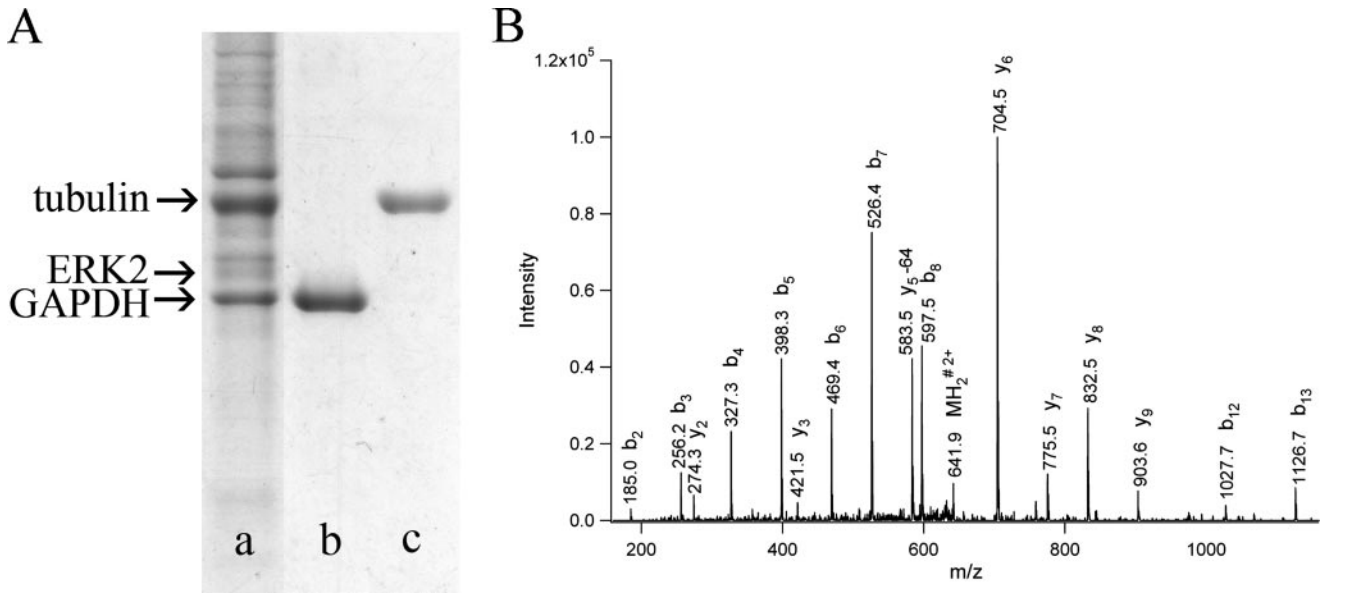

FIGURE 4. **Identification of ERK2 as an interacting partner of TPPP in bovine brain extract.** *A*, SDS/PAGE analysis of the proteins bound to the TPPP affinity column. *Lane a*, TPPP-binding proteins eluted from the column; *lane b*, 1.5 μg of GAPDH, and *lane c*, 1.5 μg of tubulin controls. *B*, ERK2 (NCBI acc. NP_786987) identified from CID of *m/z* 651.0 (2+) matching peptide sequence Ac-AAAAAAGAGPEM(ox)VR (2–15). The b and y ions represent N- and C-terminal fragment ions (38), water loss is marked as #, −64 stands for methane sulfenic acid (CH_3SOH) loss.

ments the concentration of ERK2 added to TPPP was reduced which resulted in the incorporation of 1.3 mol P/mol protein. This partially phosphorylated TPPP exhibited low tubulin polymerization activity (Fig. 5*D*). TEM showed that, in sharp contrast to the control, the sample mainly consists of thread-like oligomers, which form a loosely arranged network instead of densely packed knobs (Fig. 6*C*). We conclude that the phosphorylation strongly impedes the ability of TPPP to promote the formation and bundling of intact MTs, as well as to mediate the formation of large tubulin/TPPP aggregates.

DISCUSSION

Previous data, based on the co-purification of TPPP with Cdk5 and on the *in vitro* phosphorylation of three selected peptides by Cdk5, suggested that TPPP could be a phosphoprotein (15). In this work we identified the specific sites targeted by protein kinases involved in brain signaling processes. Ser/Thr-Pro motifs were found to be phosphorylated by both ERK2 (Ser^{18} and Ser^{160}) and Cdk5 (Thr^{14}, Ser^{18}, and Ser^{160}). It should be noted, that from the stoichiometry of phosphate incorporation (see Fig. 1) as well as from the bioinformatic prediction, three phosphorylation sites can be inferred for ERK2 (see Table 3). Thus, it is likely that Thr^{14} is also phosphorylated by ERK2, although the modification of this residue was not found by MS. Cdk5 and ERK1/2 share common sites in the tau protein (29); therefore, the cross-talk between these two kinases may occur in the case of TPPP phosphorylation as well. In addition, we found that TPPP was phosphorylated by PKA at Ser^{32}, Thr^{92}, and Ser^{159}. The fact that the truncated Δ3-43TPPP carrying Ser^{160} as potential phosphorylation site was modified only to a stoichiometry of 0.4–0.5 mol P/mole protein, suggests that the major sites of these kinases are localized in the N-terminal region. This idea was further supported by the *in vivo* phosphorylation data from our and other laboratories. We isolated TPPP from bovine brain, and identified the phosphorylated amino acid residues as Thr^{12}, Ser^{16}, and Ser^{30}. Recent proteomic analysis of *in vivo* phosphorylated human and mouse synaptic proteins (30–32) identified the same sites although there is a 1 or 2 amino acids shift between the sequences (Fig. 3). These sites of TPPP obtained by prediction as well as identified *in vitro* and *in vivo* (see Table 3) are the major targets of the kinases in the brain.

The N-terminal tail of TPPP (1–52 amino acids) was predicted to be completely disordered (8). The amino acid sequence of disordered proteins and protein regions is considered to be much less conservative than that of the structured ones (33, 34). Indeed, in the polypeptide sequences of vertebrate TPPPs, we found 25% identity between mammals and fishes in the N-terminal segment as compared with 75% identity in the C-terminal part (data not shown). However, the putative phosphorylation sites in the more variable N-terminal region are maintained during evolution (Fig. 3) indicating a physiological role for the phosphorylation of these residues.

Interestingly, Ser^{159}/Ser^{160} of bovine and human TPPP was not found to be phosphorylated *in vivo*. As demonstrated in Fig. 3*B*, the neighboring sequence (163–187 amino acids) has high homology with the tubulin binding domain of tau protein. It is possible that in the intracellular milieu these sites are masked by the association of tubulin/MT to TPPP.

All of these observations suggest the modulation of TPPP activity by phosphorylation. It is likely that in this process ERK2 plays a dominant role because of its direct binding to TPPP. In fact, by MotifScan we identified two regions of TPPP that resemble the ERK docking site called D domain (28). Although it is not known whether all ERK-interacting molecules have D domains, the existence of such a region together with our affinity binding experiment indicate that ERK2 is, indeed, a potential interacting partner and regulator of TPPP.

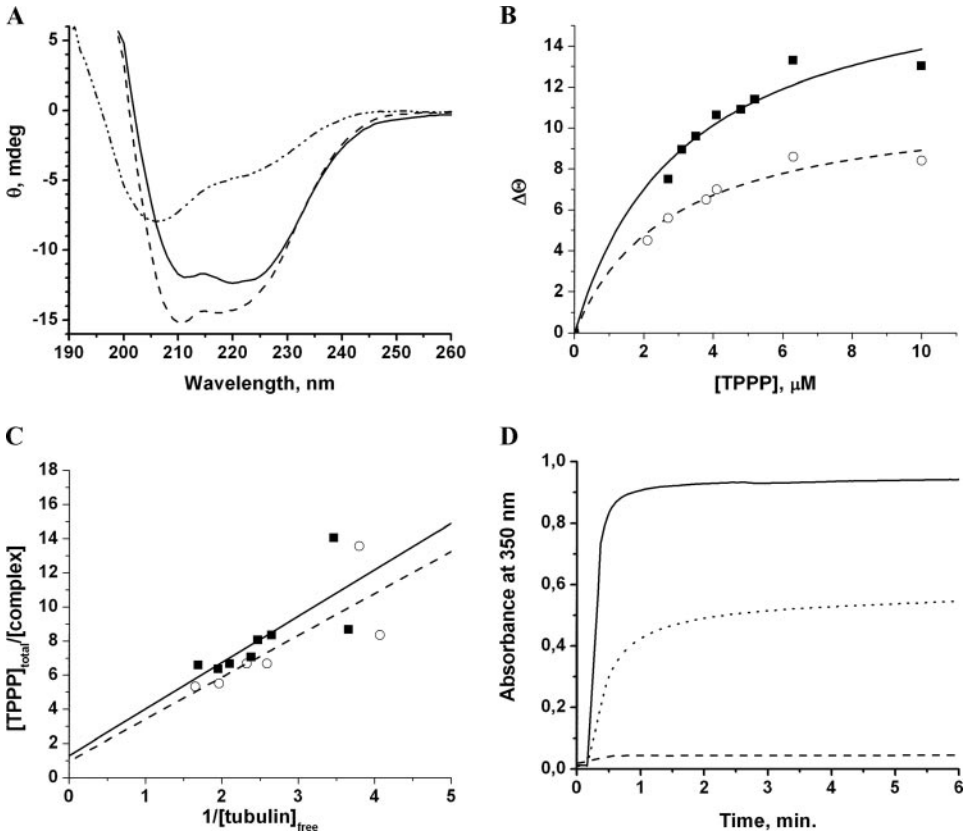

FIGURE 5. Effect of phosphorylation on the interaction of tubulin and TPPP (*A*, *B*, *C*) and on the TPPP-promoted tubulin polymerization (*D*). *A*, CD spectra of TPPP (*dash-dot-dot line*), the mixtures of tubulin and TPPP (*solid line*), of tubulin and ERK2-phosphorylated TPPP (*dashed line*). Final concentrations were 5 μM and 1 μM for TPPP and tubulin, respectively. The stoichiometry of phosphorylation was 2.9 mol P/mol protein. *B*, titration of 1 μM tubulin with non-phosphorylated (■, *solid line*) and phosphorylated (○, *dashed line*) TPPP. The difference ellipticities at 207 nm calculated from the ellipticities measured with the mixture of the two proteins and with the individual proteins were plotted as a function of the concentration of TPPP. The stoichiometry of phosphorylation was 2.9 mol P/mol protein. *C*, plots of the data of Fig. 5*B* according to Wu and Hammes (39). K_d values and the stoichiometries of the complexes obtained from the slope and the intercept on the ordinate, respectively, are 2.7 μM and 1.3, and 2.5 μM and 1.0, for the unphosphorylated and phosphorylated TPPP, respectively. *D*, tubulin polymerization induced by addition of TPPP before and after phosphorylation. Final concentrations were 7 μM tubulin and 3 μM TPPP (*solid line*) or 3 μM TPPP phosphorylated by ERK2 to the stoichiometry 2.9 mol of P/mol protein (*dashed line*) or 1.3 mol P/mol protein (*dotted line*).

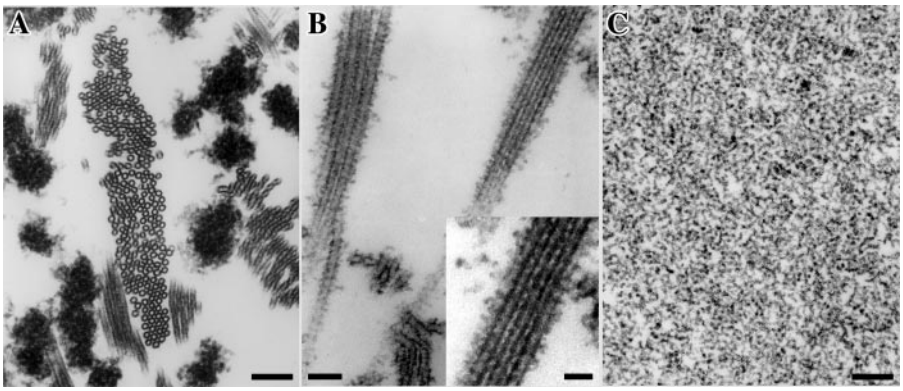

FIGURE 6. TEM images of the TPPP-induced tubulin assemblies before (*A*, *B*) and after phosphorylation (*C*) with ERK2 (1.3 mol of P/mol protein). *A* and *B*, bundles of MTs sectioned at different angles and thread-like oligomers aggregated into dense knobs are shown. The MTs are frequently covered by tiny projections and periodically arranged dense particles (*B*), which form cross-links between MTs (see *inset* in *panel B*). *C*, sample prepared with phosphorylated TPPP contains loosely arranged oligomeric threads. *Bars*, 200 nm in *A* and *C*; 100 nm in *B* and 50 nm in the *inset* in *B*.

In the present report we provided evidence for the inherent ability of TPPP to induce self-assembly of MAP-free tubulin, and for its extensive bundling activity (Fig. 6, *A* and *B*), which is a MAP-like function, similar to that of tau or MAP2 proteins in brain. The resistance of TPPP-bundled MTs against anti-microtubular agents was recently reported in human cells (3) suggesting the potential physiological role of this protein in the stabilization of the microtubular network.

Our quantitative data showed that the dissociation constants and the stoichiometries for the complexes of tubulin and TPPP as well as of tubulin and phosphorylated TPPP (2–3 mol P/mol protein) did not differ significantly; however, the secondary structural changes induced by the complex formation were found to be distinct (Fig. 5, *B* and *C*). Therefore, it is likely that the phosphorylation resulted in some structural changes in the recognition domain(s) of TPPP. As a consequence of the perturbation of the binding interface by phosphorylation, a dramatic alteration in the tubulin polymerization promoting potency of TPPP was detected (Fig. 5*D*). In fact, we found that the phosphorylation of TPPP by ERK2 (or by Cdk5) but not by PKA, blocks (Fig. 5*D*) the MT assembling activity of TPPP. A plausible explanation of this finding is that the phosphorylated TPPP is unable to induce appropriate conformational changes required for the assembly of tubulin dimers into protofilaments and tubes. Our TEM analysis revealed that limited phosphorylation of TPPP by ERK2 (1.3 mol P/mol protein incorporated) exerted on one hand, significant inhibitory effect on the MT assembling activity of TPPP; on the other hand, it inhibited the formation of large amorphous protein aggregates (Fig. 6*C*). Because our recent immunofluorescent data on HeLa cell and immunohistochemistry results on human brain samples from patients suffering in synucleinopathies provided evidence for the co-enrichment of TPPP with tubulin in aggresome, Lewy body and other inclusions (3, 5, 8), one can hypothesize that within these structures the TPPP molecules are dominantly in unphosphorylated form, and suggest possible pathological relevance of the post-translational modification of TPPP.

Cdk5 may have the same effect as ERK2 since it phosphorylates identical sites in TPPP. Because of the distinct specificity, PKA has a different substrate recognition preference: it predominantly phosphorylates Ser^{32} in the KRLS motif. The phosphorylation of TPPP at this site occurs *in vivo* and may have some important function but according to our *in vitro* results it has no significant effect on the tubulin/MT system. Therefore, we suggest that the functional consequences of phosphorylation of Thr^{14} and/or Ser^{18} residues but not Ser^{32} in the N-terminal region of TPPP play a crucial role in the regulation of the MT assembly and stabilization of the microtubular network. Because the phosphorylation pattern of a protein with multiple phosphorylation sites depends on the coordinated action of protein kinases and phosphatases (35) further investigations are needed to clarify the detailed regulatory mechanisms modulating the functions of TPPP. The significance of the phosphatases in the regulation has been underlined by the example of tau protein that is dephosphorylated by several protein phosphatases (36, 37).

Acknowledgment—Kromat Ltd. is greatly acknowledged for providing the use of an Agilent 1100 nanoLC-XCT Plus IonTrap system.

REFERENCES

1. Tirián, L., Hlavanda, E., Oláh, J., Horváth, I., Orosz, F., Szabó, B., Kovács, J., Szabad, J., and Ovádi, J. (2003) *Proc. Natl. Acad. Sci. U. S. A.* **100,** 13976–13981
2. Hlavanda, E., Kovács, J., Oláh, J., Orosz, F., Medzihradszky, K. F., and Ovádi, J. (2002) *Biochemistry* **41,** 8657–8664
3. Lehotzky, A., Tirián, L., Tőkési, N., Lénárt, P., Szabó, B., Kovács, J., and Ovádi, J. (2004) *J. Cell Sci.* **117,** 6249–6259
4. Vincze, O., Tőkési, N., Oláh, J., Hlavanda, E., Zotter, Á., Horváth, I., Lehotzky, A., Tirián, L., Medzihradszky, K. F., Kovács, J., Orosz, F., and Ovádi, J. (2006) *Biochemistry* **45,** 13818–13826
5. Kovács, G. G., László, L., Kovács, J., Jensen, P. H., Lindersson, E., Botond, G., Molnár, T., Perczel, A., Hudecz, F., Mező, G., Erdei, A., Tirián, L., Lehotzky, A., Gelpi, E., Budka, H., and Ovádi, J. (2004) *Neurobiol. Dis.* **17,** 155–162
6. Oláh, J., Tőkési, N., Vincze, O., Horváth, I., Lehotzky, A., Erdei, A., Szájli, E., Medzihradszky, K. F., Orosz, F., Kovács, G. G., and Ovádi, J. (2006) *FEBS Lett.* **580,** 5807–5814
7. Lindersson, E., Lundvig, D., Petersen, C., Madsen, P., Nyengaard, J. R., Hojrup, P., Moos, T., Otzen, D., Gai, W. P., Blumbergs, P. C., and Jensen, P. H. (2005) *J. Biol. Chem.* **280,** 5703–5715
8. Orosz, F., Kovács, G. G., Lehotzky, A., Oláh, J., Vincze, O., and Ovádi, J. (2004) *Biol. Cell* **96,** 701–711
9. Murray, A. W. (1998) *Cell* **92,** 157–159
10. Veeranna, G. J., Shetty, K. T., Takahashi, M., Grant, P., and Pant, H. C. (2000) *Brain Res. Mol. Brain Res.* **76,** 229–236
11. Sharma, P., Veeranna Sharma, M., Amin, N. D., Sihag, R. K., Grant, P., Ahn, N., Kulkarni, A. B., and Pant, H. C. (2002) *J. Biol. Chem.* **277,** 528–534
12. Langeberg, L. K., and Scott, J. D. (2005) *J. Cell Sci.* **118,** 3217–3220
13. Scott, J. D., Stofko, R. E., McDonald, J. R., Comer, J. D., Vitalis, E. A., and Mangili, J. A. (1990) *J. Biol. Chem.* **265,** 21561–21566
14. Hausken, Z. E., Coghlan, V. M., Hastings, C. A., Reimann, E. M., and Scott, J. D. (1994) *J. Biol. Chem.* **269,** 24245–24251
15. Takahashi, M., Tomizawa, K., Ishiguro, K., Sato, K., Omori, A., Sato, S., Shiratsuchi, A., Uchida, T., and Imahori, K. (1991) *FEBS Lett.* **289,** 37–43
16. Martin, C. P., Vazquez, J., Avila, J., and Moreno, F. (2002) *Biochim. Biophys. Acta* **1586,** 113–122
17. Na, C. N., and Timasheff, S. N. (1986) *Biochemistry* **25,** 6214–6222
18. Bradford, M. M. (1976) *Anal. Biochem.* **72,** 248–254
19. Laemmli, U. K. (1970) *Nature (Lond.)* **227,** 680–688
20. Witt, J. J., and Roskoski, R. (1975) *Anal. Biochem.* **66,** 253–258
21. Nestler, E. J., and Greengard, P. (1983) *Nature* **305,** 583–588
22. Ficarro, S. B., McCleland, M. L., Stukenberg, P. T., Burke, D. J., Ross, M. M., Shabanowitz, J., Hunt, D. F., and White, F. M. (2002) *Nat. Biotech.* **20,** 301–305
23. Thompson, A. J., Hart, S. R., Franz, C., Barnouin, K., Ridley, A., and Cramer, R. (2003) *Anal. Chem.* **75,** 3232–3243
24. Larsen, M. R., Thingholm, T. E., Jensen, O. N., Roepstorff, P., and Jorgensen, T. J. D. (2005) *Mol. Cell Proteomics* **4,** 873–886
25. Obenauer, J. C., Cantley, L. C., and Yaffe, M. B. (2003) *Nucleic Acids Res.* **31,** 3635–3641
26. Thompson, J. D., Higgins, D. G., and Gibson, T. J. (1994) *Nucleic Acids Res.* **22,** 4673–4680
27. Covey, T. R., Sushan, B. I., Bonner, R., Shroder, W., and Hucho, F. (1991) *Methods in Protein Sequence Analysis* (Jörnvall, H., Höög, J. O., and Gustavsson, A. M., eds) pp. 411–447, Birkhauser Verlag Basel
28. Tanoue, T., and Nishida, E. (2003) *Cell. Signal.* **15,** 455–462
29. Jamsa, A., Backstrom, A., Gustafsson, E., Dehvari, N., Hiller, G., Cowburn, R. F., and Vasange, M. (2006) *Biochem. Biophys. Res. Commun.* **345,** 324–331
30. DeGiorgis, J. A., Jaffe, H., Moreira, J. E., Carlotti, C. G., Leite, J. P., Pant, H. C., and Dosemeci, A. (2005) *J. Proteome Res.* **4,** 306–315
31. Collins, M. O., Yu, L., Coba, M. P., Husi, H., Campuzano, I., Blackstock, W. P., Choudhary, J. S., and Grant, S. G. (2005) *J. Biol. Chem.* **280,** 5972–5982
32. Trinidad, J. C., Specht, C. G., Thalhammer, A., Schoepfer, R., and Burlingame, A. L. (2006) *Mol. Cell. Proteomics* **5,** 914–922
33. Chen, J. W., Romero, P., Uversky, V. N., and Dunker, A. K. (2006) *J. Proteome Res.* **5,** 879–887
34. Chen, J. W., Romero, P., Uversky, V. N., and Dunker, A. K. (2006) *J. Proteome Res.* **5,** 888–898
35. Ulloa, L., Dombrádi, V., Diaz-Nido, J., Szűcs, K., Gergely, P., Friedrich, P., and Avila, J. (1993) *FEBS Lett.* **330,** 85–89
36. Liu, F., Grundke-Iqbal, I., Iqbal, K, and Gong, C. X. (2005) *Eur. J. Neurosci.* **22,** 1942–1950
37. Wang, J. Z., Grundke-Iqbal, I., and Iqbal, K. (2007) *Eur. J. Neurosci.* **25,** 59–68
38. Biemann, K. (1990) *Methods Enzymol.* **193,** 886–887
39. Wu, C. W., and Hammes, G. G. (1973) *Biochemistry* **12,** 1400–1408